

Removal of cefixime from aqueous solutions by the biosorbent prepared from pine cones: kinetic and isotherm studies

Dariussh Naghipour^a, Abdoliman Amouei^{b,c,*}, Kamran Taher Ghasemi^d, Kamran Taghavi^e

^aResearch Center of Health and Environment, Guilan University of Medical Sciences, Rasht, Iran, email: dr.naghipour@gmail.com (D. Naghipour)

^bSocial Determinants of Health Research Center, Health Research Institute, Babol University of Medical Sciences, Babol, Iran, Tel. +9822344366; Fax: +9822334367; email: iamouei1966@gmail.com (A. Amouei)

^cEnvironmental Health Research Center (EHRC), Health Research Institute, Babol University of Medical Sciences, Babol, Iran

^dMSc of Environmental Health, Guilan University of Medical Sciences, Rasht, Iran, email: taherghasemi@yahoo.com (K.T. Ghasemi)

^eDepartment of Environmental Health, Guilan University of Medical Sciences, Rasht, Iran, email: taghavi_k@yahoo.com (K. Taghavi)

Received 8 October 2019; Accepted 14 May 2020

ABSTRACT

The bio-char prepared from pine cones was used to remove cefixime (CFX) from aqueous solutions. The influence of some parameters including pH (2–12), contact time (0 to 120 min), initial concentration of CFX (10, 50, and 100 mg L⁻¹), adsorbent dose (0.1 to 2.5 g L⁻¹), temperature (10°C to 50°C) was evaluated. The pine cones pieces were washed with the distilled water, dried, crushed, and sieved to provide a particle size of 100–250 nm. For carbonization, the dried raw material was put into a stainless steel reactor and heated in an electrical furnace at 20°C per min and maintained at 460°C for 2 h. After carbonization, the samples were washed with distilled water and then dried at 105°C for 12 h, and were used as adsorbent. The specific surface area, total pore volume, and mean pore diameter of the biosorbent were determined to be 789 m² g⁻¹, 0.373 cm³ g⁻¹, and 1.89 nm, respectively. In the optimum conditions (pH = 6.3, initial concentration of CFX = 50 mg L⁻¹, contact time = 90 min, and adsorbent dose = 2 g L⁻¹), the removal efficiency was 92%. The adsorption isotherm of CFX follows the Langmuir model. The kinetic study confirmed that the adsorption process fits with the pseudo-second-order reaction. The thermodynamic study indicated that the adsorption of CFX by the bio-char is feasible, spontaneous, and exothermic. This study represents that the biosorbent prepared from the pine cones can be used as an appropriate and cost-effective adsorbent for the removal of CFX from aqueous solutions and hospital wastewater.

Keywords: Cefixime; Adsorption; Pine cones; Bio-char; Kinetics; Isotherms

1. Introduction

Antibiotics are broadly used for remedy of diseases in humans, animals, and plants [1,2]. These compounds are drugs that prohibit the growth of the pathogenic agents [3]. Disposal of wastewaters from residential places, hospitals, veterinary, and pharmaceutical centers to the receiving environments has many impacts on human and

environmental health [4]. These wastewaters can cause potential risks to human and other living things due to including a number of different pharmaceutical compounds such as antibiotics [5,6]. Nearly 30% to 90% of the antibiotic compounds consumed by humans and animals are not completely metabolized and dispose to the environment [7]. These toxic compounds are not biodegradable using microorganisms [8,9]. Some mutagenic and carcinogenic effects of

* Corresponding author.

these materials have been reported in many investigations [10,11]. On the other hand, conventional wastewater treatment plants can remove less than 60% of antibiotics and other drugs from municipal wastewater [12,13].

Cefixime (CFX) belongs to the group of cephalosporines and is an antibiotic that used widely for treating of several diseases [14]. This compound can be used to remove different disease-causing bacteria, including *Staphylococcus ureous*, *Streptococcus pneumonia*, *Escherichia coli*, and etc. [15]. The chemical formula and molecular weight of CFX are $C_{16}H_{15}N_5O_7S_2 \cdot 3H_2O$ and 453.5 g mol^{-1} , respectively (Fig. 1). Isoelectric point of this antibiotic (pK_a) is 4.7 [16]. The maximum contamination level of CFX in water resources as an organic pollutant is $5 \mu\text{g L}^{-1}$ [14]. Due to the widespread use of this antibiotic in the treatment of the different diseases in humans and animals, CFX plays an important role in environmental pollution and even at low concentrations may cause resistance to pathogenic bacteria in the environment [11,14].

There are several methods to remove antibiotic compounds from environments, including advanced oxidation processes [17–19], ion exchange [20], membrane technologies [4], biological treatment methods, and adsorption process [13,21,22]. Biological treatment process is not appropriate to degrade antibiotics because of these materials destruct the microorganisms involved in biological wastewater treatment [23,24]. On the other hand, the use of membrane and advanced oxidation techniques in a large scale are very expensive [25,26].

The adsorption process is more efficient than other physical methods for the removal of antibiotics from pharmaceutical and hospital wastewaters [27,28]. This process has many advantages including simple design and implementation, non-toxic residual production, and the efficient removal of pollutants for recovery [16,21]. The efficiency of the adsorption process depends on several parameters such as the adsorbent type, properties of the pollutant, and the characteristics of the wastewater [29,30].

Nowadays, inorganic minerals [16,31,32], agricultural and natural wastes [33,34] are widely used as an adsorbent to remove various organic and inorganic pollutants from aqueous solutions and wastewaters. Rasoulifard et al. [15] have used a hardened paste of Portland cement (HPPC) and the modified HPPC with perlite for removal of CFX from aqueous solutions. In this study, the effects of adsorbate concentration, adsorbent dosage, type of adsorbent, contact time, and pH on CFX adsorption were investigated.

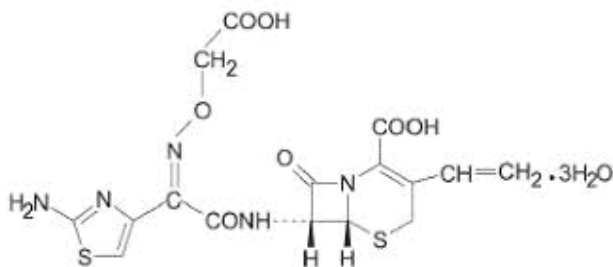


Fig. 1. Chemical structure of CFX [15].

The results showed that HPPC and modified HPPC were efficient adsorbents for CFX removal [16]. In another study, adsorption of CFX antibiotic from aqueous solution was studied by activated carbons (ACs) derived from date press cake (DPC) and an agro-industrial waste (AIW). Both of these materials successfully adsorbed CFX from aqueous solution with maximum monolayer adsorption capacities of 557.9 and 571.5 mg g^{-1} , respectively (35).

Pine tree (*Pinus roxburghii*) is one of the most planted trees of Iran, which is cultivated in different places in this country. Therefore, in this study, the pinecones were used for the preparation of the adsorbent, and finally, the prepared bio-char was used as a natural and environmental friendly adsorbent to remove CFX from aqueous solutions and hospital wastewaters.

The aim of this study, evaluating the effect of the various parameters including pH of solution, contact time, adsorbent dose, initial concentration of CFX, and solution temperature on the adsorption efficiency, thermodynamic study, and determination of the appropriate isotherms and kinetic models.

2. Materials and methods

2.1. Chemicals

In this study, all the chemicals used were analytical grade and all solutions were prepared with distilled waters. CFX (99.6%, standard grade) used was obtained from Merck Co., Germany. The pH of the solutions was adjusted by hydrochloric acid (37% purity) and sodium hydroxide (48% purity).

2.2. Preparation of the bio-char prepared from pine cones

The pine cones pieces were washed with distilled water several times to remove dust and other impurities and dried, crushed, and sieved to provide a particle size of 100–250 nm. Then, the samples were placed in a vertical stainless-steel reactor under high purity nitrogen (99.99%) at a flow rate of $350 \text{ cm}^3 \text{ min}^{-1}$ and heated in an electrical furnace at 20°C per min and maintained at 460°C for 2 h [35]. After carbonization, the samples were washed with distilled water and then dried at 105°C for 12 h. The obtained material, hereafter named activated or bio-char carbon was kept in tightly closed bottles and are being used as adsorbent. The yield obtained for the preparation of the bio-char was calculated as follow:

$$\text{Yield (\%)} = \frac{W_c}{W_r} \times 100 \quad (1)$$

where W_c is dry weight (g) of the bio-char and W_r is dry weight of raw pine cones.

2.3. Determination of physical and chemical characteristics of the pine cones bio-char

Specific surface area and pore volumes of the adsorbent were analyzed by the Brunauer–Emmet–Teller (BET)

method. Fourier transform infrared (FTIR) spectroscopy (Vertex 70, Bruker, Germany) was used in the wavenumber range of 4,000–500 cm^{-1} to analyze the functional groups of the bio-chars. The morphology of the selected bio-char before and after CFX adsorption was analyzed by a field emission scanning electron microscopy (FESEM) (Hitachi, S-3000N), using an accelerating voltage of 20 kV.

2.4. Determining the pH_{pzc} of the adsorbent prepared from the pine cones

The pH_{pzc} of the prepared bio-char was determined using the direct pH measurement method. Fifty milliliters of the 0.1 M NaCl solution was poured in each 150 mL Erlenmeyer flask and the pH was adjusted in the 2–12 range using NaOH and HCl. The adsorbent (0.04 g) was then added to each solution, the Erlenmeyer flasks were closed with screw caps and stirred for 40 h using an electric stirrer, and the final pH was measured and its curve was drawn against the initial pH. The point where the bisector intersected the curve was determined as the pH_{pzc} of the bio-char.

2.5. Adsorption experimentations and data analysis

In each test, 50 mL of the CFX with different concentrations (10, 50, and 100 mg L^{-1}) was transferred into the Erlenmeyer flasks. The pH of the solution was adjusted using hydrochloric acid or sodium hydroxide 0.1 N. The definite doses of the pine cones bio-char (0.1, 0.25, 0.5, 1, 1.5, 2, 2.5, and 3 g) were added into the solution and mixed at 150 rpm. After completely mixing at a specific time, the solution was centrifuged at 5,000 rpm, and the CFX concentration in the solution was analyzed by Hack model of DR5000 spectrophotometer at the wavelength 221 nm and measured using a standard curve. All experiments were repeated three times in order to obtain accurate results. The capacity of adsorbents for the adsorption of CFX (q_e and q_t) and removal efficiency (RE) of CFX were calculated as follows:

$$q_e = \frac{(C_i - C_e) \times V}{W} \quad (2)$$

$$q_t = \frac{(C_i - C_t) \times V}{W} \quad (3)$$

$$\text{RE} = \frac{(C_i - C_e)}{C_i} \times 100 \quad (4)$$

where C_i , C_e , and C_t are the initial, equilibrium, and at time t concentrations of CFX (mg L^{-1}), respectively, V is the volume of suspension (L), and W is the dry weight of the adsorbent in suspension (g).

In the adsorption kinetics experiment, the data were fitted using a pseudo-first-order (PFO) model (Eq. (5)), and a pseudo-second-order (PSO) model (Eq. (6)).

$$q_t = q_e (1 - e^{-k_1 t}) \quad (5)$$

$$q_t = \frac{k_2 q_e^2 t}{1 + k_2 q_e t} \quad (6)$$

where k_1 (h^{-1}) and k_2 ($\text{g mg}^{-1} \text{h}^{-1}$) are the rate constants of the PFO and PSO models, respectively. Additionally, q_e (mg g^{-1}) is the sorption capacity at the equilibrium time, and I is the intercept reflecting the extent of the boundary layer thickness [36].

The Langmuir (Eq. (8)), Freundlich (Eq. (9)), and Temkin (Eq. (10)) adsorption models were fitted to the data of the adsorption isotherms.

$$q_e = \frac{q_{\text{max}} \times K_L \times C_e}{1 + K_L \times C_e} \quad (7)$$

$$q_e = K_F \times C_e^{1/n_f} \quad (8)$$

$$q_e = \frac{RT}{B_T} \text{Ln } A_T + \frac{RT}{B_T} \text{Ln } C_e \quad (9)$$

where C_e (mg L^{-1}) is the tetracycline concentration in the solution phase, K_L (L mg^{-1}) is the Langmuir sorption coefficient, q_{max} (mg g^{-1}) is the maximum sorption capacity, and K_F ($\text{mg}^{1-n} \text{L}^n \text{g}^{-1}$) and n are the sorption and nonlinear coefficients in the Freundlich equation, respectively. Additionally, K_T (L mg^{-1}) is the Tempkin constant that corresponds to the maximum binding energy. Moreover, T ($^{\circ}\text{K}$) and R ($8.314 \text{ J mol}^{-1} \text{ K}^{-1}$) are the absolute temperature and universal gas constant, respectively, while B_T is obtained after solving the Temkin equation.

3. Results and discussion

3.1. Yield, textural, and chemical surface characterization of the adsorbent

In this study, the yield value of the prepared bio-char from dry raw pine cones was 35.5% at 460°C for 2 h. Similar, yields were found by other researchers who prepared activated carbons from agro-industrial wastes. Nazari et al. [28] reported a 41.3% yield value for carbonized material (CM) obtained from the Walnut shell through heating at 450°C for 1 h. Martins et al. [37] obtained 30.54% CM yield derived from Macadamia nutshells. After activation, the yield value is greatly reduced [38]. The loss in activated carbon weight could be related to the temperature, processing time, and type of the raw material [29].

The specific surface area ($a_{\text{s,BET}}$), total pore volume (V_T), and mean pore diameters (D_p) of the produced bio-char were determined 789 $\text{m}^2 \text{g}^{-1}$, 0.373 $\text{cm}^3 \text{g}^{-1}$, and 1.89 nm, respectively. The FTIR spectrum of the bio-char are shown in Fig. 2. The bands in the 1,000–1,300 cm^{-1} range can be attributed to the C–C and C–O vibrations in acids, alcohols, phenols, ethers, and esters [29,32]. The broad peak at 3,430.45 cm^{-1} is related to the O–H strengthening and vibration of carboxyl and phenol functional groups or adsorbed water, and the asymmetric peak shape is characteristic of hydrogen bonding [33]. The peak at 1,085.76 cm^{-1} indicates the presence of amine functional group on the adsorbent surface [14]. In

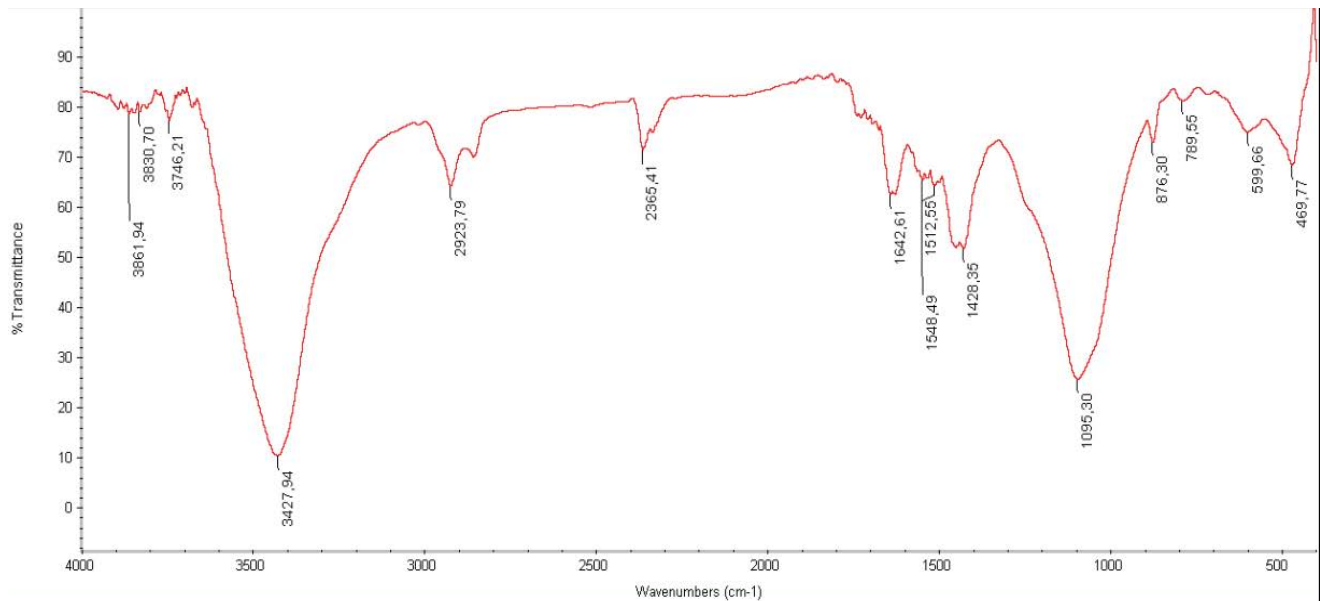


Fig. 2. FTIR spectrum of the bio-char.

Table 1, the physical properties of some biosorbents derived agro-industrial wastes were presented.

SEM images of the bio-char prepared from the pine cone before and after the CFX adsorption were presented in Figs. 3 and 4, respectively. According to Fig. 4, the pores of the adsorbent after adsorption, filled with CFX molecules.

3.2. Determination of point of zero charge (pH_{pzc})

The point of zero charge in any adsorbent is a point that an adsorbent has zero potential charges on its surface [29]. In this study, the pH_{pzc} of the surface of the bio-char was determined to be 6.5 (Fig. 5). When the pH of the solution is lower than the pH_{pzc} , the solution donates more protons to the adsorbent, and so the adsorbent surface is positively charged (cationic behavior). Conversely, if the pH of the solution is more than the pH_{pzc} , the functional groups in the adsorbent surface is negatively charged (anionic behavior) [15,31].

3.3. Effect of pH on CFX adsorption

In this study, the effect of initial pH on the adsorption of CFX was investigated. According to Fig. 6, the maximum adsorption capacity approximately 115 mg g^{-1} , and the maximum removal efficiency of CFX (92%) is obtained at a pH value of 6.3. According to the CFX isoelectric point ($pK_a = 4.7$), this compound is non-ionized form at this point and so has a higher negative charge at $pH > 4.7$ and a higher positive charge at $pH < 4.7$. On the other hand, pH_{pzc} of the surface of the bio-char is 6.5. Therefore, at the pH solution between 4.7 and 6.5 ($pH = 6.3$), the removal efficiency of CFX by the bio-char is maximum.

At acidic ($pH < 4.7$) and alkaline ($pH > 7$) conditions, the CFX removal gradually decreases. It can be attributed to the fact that at $pH < 4.7$, the positive functional groups on the surface of the adsorbent and the CFX solution is dominant. This phenomenon leads to a removal deficiency due to an increase of the repulsive forces between the positive

Table 1
Comparison of the different adsorbents as physical property and adsorption capacity

Sorbent	Adsorbate	pH	t (min)	Dose (g L^{-1})	BET ($\text{m}^2 \text{g}^{-1}$)	q_m (mg g^{-1})	Reference
Lotus stacks AC	Norfloxacin	6	100	0.4	1,031.8	66.2	[22]
Walnut shell AC	Cephalexin	6.5	120	0.6	1,452	219	[28]
Date press cake	Cefixime	4	45	1	2,623	557.9	[38]
MgO nanoparticle	Cephalosporines	9	10	0.5	48	526.3	[39]
Carbon nanotube	Cephalosporines	5	60	1.5	–	38.5	[40]
Tomato AC	Tetracycline	5.7	180	0.1	1,093	500	[41]
Rice straw AC	Tetracycline		60	0.8	21.69	316	[36]
Alligator weed AC	Cephalexin	6	240	1.6	736.3	35	[42]
Orange peel AC	Emerging pollutants	7	460	0.5	304	11	[43]
Pine cone AC	Cefixime	6.3	90	2	798	115	Present study

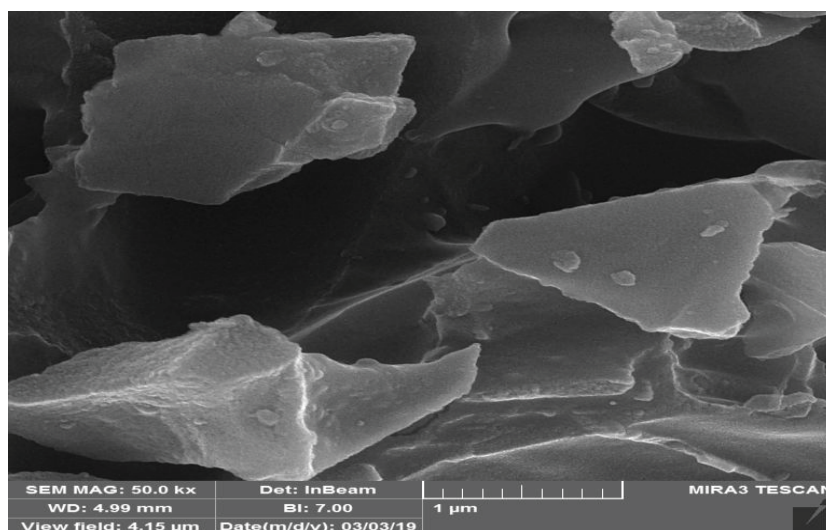


Fig. 3. SEM image of the pine cones bio-char before the CFX adsorption.

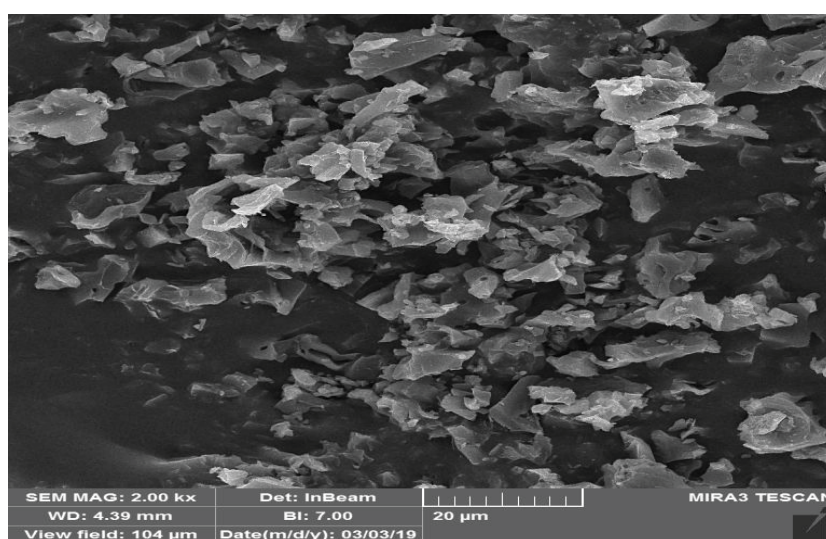


Fig. 4. SEM image of the pine cones bio-char after the CFX adsorption.

charges of the adsorbent surface and CFX solution [10,38]. At $\text{pH} > 7$, the negative functional groups of CFX solution are predominant and the negative charges on the surface of the bio-char due to the deprotonation (obtaining OH^-) increase, which result in the repulsive forces between the negative charges of the solution and the bio-char surface increases. As a result, the adsorption of CFX decreased. It is notable that some negative and positive functional groups can simultaneously exist on the surface of the adsorbent while the surface charge of the adsorbent may be predominantly positive or negative [36,37].

3.4. Effect of adsorbent dose on CFX adsorption

The influence of adsorbent dosage on the adsorption capacity and CFX removal efficiency from aqueous solution is presented in Fig. 7. It shows that the removal of CFX

increases with the increase in the adsorbent dosage up to a certain amount (2 g) and then it remains almost constant. An increase in the removal efficiency with adsorbent dosage can be related to an increase in the surface area and the availability of more adsorption sites [15,29]. However, with the enhancement of adsorbent dose, adsorption capacity decreased considerably. The decrease in the CFX adsorption capacity with an increasing dosage of the adsorbent is essentially due to remain unsaturated sites during the adsorption process [38,41].

3.5. Effect of initial concentration and contact time on CFX adsorption

As can be seen in Fig. 8, at the lower concentration of CFX solution (10 mg L^{-1}), the removal efficiency was higher than other concentrations (50 and 100 mg L^{-1}). In this

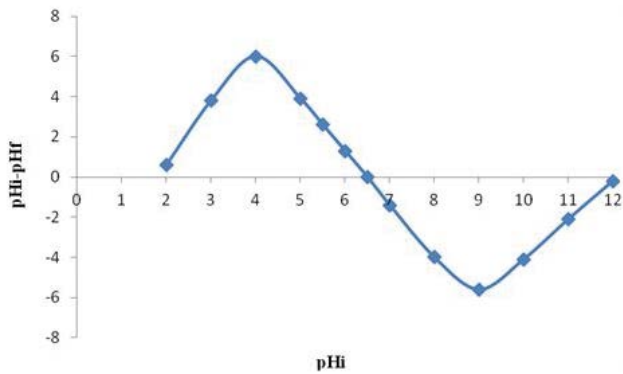


Fig. 5. Determination of the point of zero charge of the bio-char.

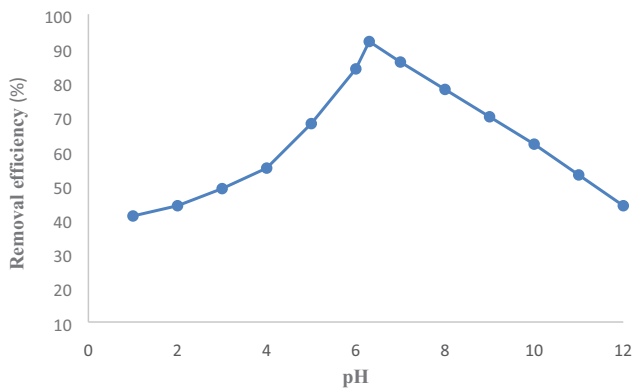


Fig. 6. Effect of pH of solution on the CFX removal efficiency ($C = 50 \text{ mg L}^{-1}$, adsorbent dose = 2 g, time = 90 min, and $T = 25^\circ\text{C}$).

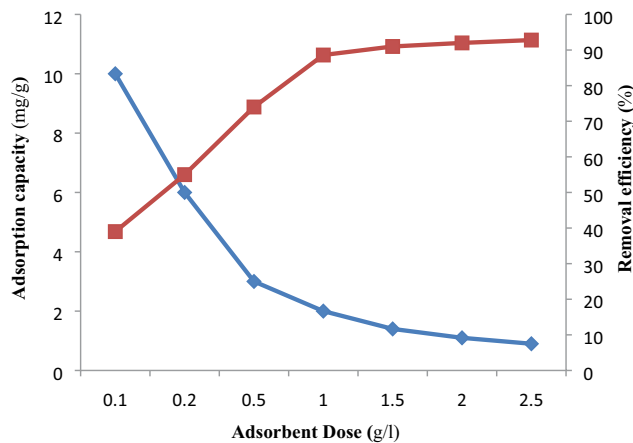


Fig. 7. Effect of adsorbent dose on the CFX removal efficiency and adsorption capacity ($C = 50 \text{ mg L}^{-1}$, $\text{pH} = 6.2$, time = 90 min, and $T = 25^\circ\text{C}$).

situation, the fraction of the initial adsorbate moles number to the number of the active site is low, and as a result, more CFX molecules can be adsorbed on the active sites of the bio-char [28,38].

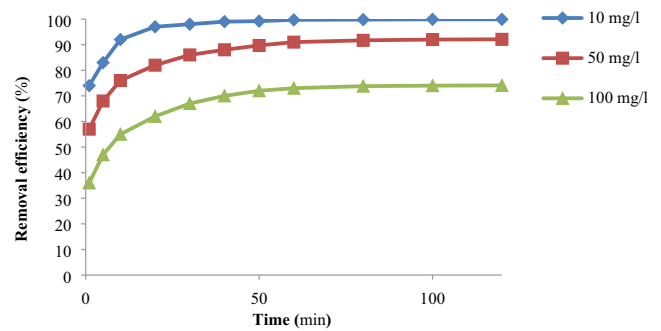


Fig. 8. Effect of the initial concentrations and contact time on the CFX removal efficiency (adsorbent dose = 2 g, $\text{pH} = 6.2$, and $T = 25^\circ\text{C}$).

Whereas in higher concentration (100 mg L^{-1}), there are not enough active sites for a large number of the CFX moles on the bio-char, so the removal efficiency of CFX decreases [32,42]. In the study, the optimum concentration was determined as 50 mg L^{-1} with the 92% removal efficiency at a contact time of 90 min. It is considered that the adsorption capacity is increasing with adsorbate concentration increase [41].

3.6. Kinetic of CFX adsorption on the bio-char

The kinetic study is useful for the understanding of the dynamic and rate of the reaction in the adsorption process [36,37]. The kinetics of any adsorption process is usually evaluated by the PFO and PSO models to fit the experimental data. The linear form of the PFO kinetic model can be presented by Eq. (5):

$$\ln(q_e - q_t) = \ln q_e - k_1 t \quad (10)$$

The PSO model is based on chemisorption on the adsorbent. The linear form of the PSO kinetic model can be expressed by the following equation:

$$\frac{t}{q_t} = \frac{1}{k_2 q_e^2} + \frac{1}{q_e} \quad (11)$$

Based on the correlation coefficients for the PFO and PSO kinetic models in concentrations 50 and 100 mg L^{-1} (Table 2), the PSO had the highest correlation coefficient and followed a straight line. Moreover, the comparison of the theoretical and experimental CFX adsorption ($q_{e, \text{cal}}$ vs $q_{e, \text{exp}}$) represents that the PSO rate is more accurate than PFO. Therefore, it can be concluded that in this experiment, the PSO is more favorable for CFX adsorption.

3.7. Adsorption isotherms of CFX on the bio-char

An adsorption isotherm describes the relationship between amount of the adsorbate substance on the adsorbent and the concentration of the adsorbate in the solution

Table 2
PFO and PSO constants and correlation coefficients for adsorption on the bio-char

C ₀ (mg L ⁻¹)	q _{e,exp} (mg g ⁻¹)	Pseudo-first-order			Pseudo-second-order		
		R ²	q _{e,cal} (mg g ⁻¹)	k ₁ (min ⁻¹)	R ²	q _{e,cal} (mg g ⁻¹)	k ₂ (g mg ⁻¹ min ⁻¹)
50	38	0.989	21.65	0.042	0.998	97.08	0.002
100	68.73	0.976	54.59	0.023	0.996	62.11	0.005

at equilibrium state. In this work, Langmuir, Freundlich, and Temkin isotherms are used to explain the equilibrium behavior in the adsorption process [37,44]. Langmuir model is valid for single-layer adsorption on the adsorbent with limited and homogeneous adsorption sites. Langmuir isotherm defined by the following equation:

$$q_e = \frac{q_{max} \times K_L \times C_e}{1 + K_L \times C_e} \tag{12}$$

where q_{max} (mg g⁻¹) is the maximum adsorption capacity; C_e (mg L⁻¹) is the equilibrium concentration; q_e (mg g⁻¹) is the equilibrium adsorption capacity, and K_L (L mg⁻¹) is the Langmuir equilibrium constant.

The Freundlich isotherm model is an empirical equation, and the model is valid for the adsorption process that occurs on heterogeneous surfaces. The Freundlich isotherm can be represented by Eq. (6):

$$q_e = K_F \times C_e^{1/n_F} \tag{13}$$

where K_F is the Freundlich equilibrium constant [mg g⁻¹ × (mg L⁻¹)^{-1/n_F}] and n_F is the dimensionless exponent of the Freundlich model.

Another isotherm in the adsorption process is Temkin model. According to this model, the heat of adsorption of all molecules in the layer decreases linearly due to adsorbent and adsorbate interaction. The equation is shown as follows:

$$q_e = \frac{RT}{B_T} \ln T_T + \frac{RT}{B_T} \ln C_e \tag{14}$$

where C_e is the concentration of CFX in equilibrium, R (8.314 j mol⁻¹ K⁻¹) is the universal gas constant, T (K) is the absolute temperature, B_T (J mol⁻¹) is the Temkin constant, and A_T (L g⁻¹) is the equilibrium binding constant. The A_T and B_T are obtained by plotting q_e vs. lnC_e.

The results of the CFX adsorption isotherm are presented in Table 3. Based on Table 3, the correlation coefficient (R²) for the Langmuir isotherm (R² = 0.990) is higher than the Freundlich (R² = 0.947) and Temkin (R² = 0.808) isotherms.

3.6. Effect of temperature on the CFX adsorption and thermodynamic studies

The effect of temperature on the removal efficiency was determined in the temperature range of 10°C–50°C (Fig. 9). Thermodynamic parameters such as Gibbs free energy (ΔG°), standard enthalpy (ΔH°), and standard entropy (ΔS°) were calculated by Eqs. (10) and (11):

$$\Delta G^\circ = \Delta H^\circ - T\Delta S^\circ \tag{15}$$

$$\ln K_L = \frac{\Delta S^\circ}{R} - \frac{\Delta H^\circ}{RT} \tag{16}$$

where R is the universal gas constant (8.314 J mol⁻¹K⁻¹), T is the absolute temperature (K), and K_L is the thermodynamic equilibrium constant, determined from q_e/C_e. ΔS° and ΔH° amounts of the sorption process were, respectively, obtained from the slope and intercept of plotting lnq_e/C_e vs. 1/T in Eq. (11), respectively. The results of the thermodynamic parameters were summarized in Table 4.

Table 3
Isotherm constants for the adsorption of CFX onto the pine cone bio-char

Isotherm models	Parameters
Langmuir	$q_e = \frac{q_m K_L C_e}{1 + K_L C_e}; R_L = \frac{1}{1 + K_L C_e}$ $q_m = 114.94 \text{ (mg g}^{-1}\text{)}, K_L = 0.25 \text{ (L mg}^{-1}\text{)}, \text{ and } R^2 = 0.992$
Freundlich	$q_e = K_F C_e^{1/n_F}$ $K_F = 41.28 \text{ (mg g}^{-1}\text{)}, n_F = 5.11, 1/n_F = 0.20, \text{ and } R^2 = 0.974$
Temkin	$q_e = \frac{RT}{B_T} \ln A_T + \frac{RT}{B_T} \ln C_e$ $A_T = 19.18, B_T = 185.41, \text{ and } R^2 = 0.808$

Table 4
Thermodynamic parameters for the adsorption of CFX onto the prepared bio-char

Temperature (K)	ΔG° (kJ mol ⁻¹)	ΔH° (kJ mol ⁻¹)	ΔS° (J mol ⁻¹ K)
283	-10,117		
293	-10,450		
303	-10,580	-6,568	13.06
313	-10,669		
323	-10,741		

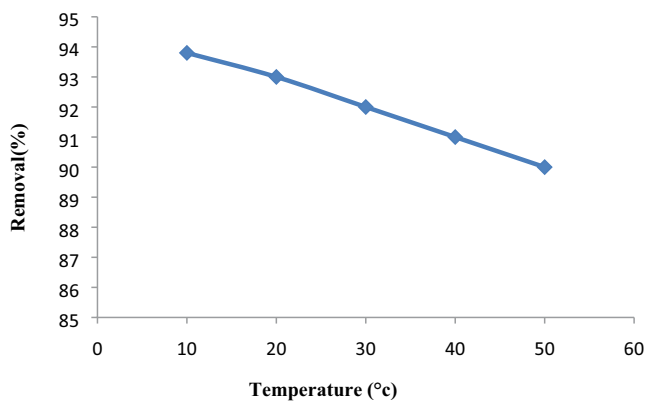


Fig. 9. Effect of temperature on the CFX removal efficiency (C = 50 mg L⁻¹, pH = 6.2, adsorbent dose = 2 g, and time = 90 min).

Based on the results, the negative values of ΔG° indicate that the sorption process was thermodynamically feasible and spontaneous. Generally, the ΔG° value is in the range of 0–20 and 80–400 kJ mol⁻¹ for physical and chemical adsorptions, respectively [41]. Therefore, the values of ΔG° indicates that the adsorption of CFX is a physiochemical mechanism. The negative and positive values of ΔH° in the adsorption process represent the exothermic and endothermic reactions, respectively [36]. So, the negative value of ΔH° in the present study is a representative of the exothermic process. In the exothermic reactions of adsorption process, the adsorption capacity and removal efficiency decrease with increasing temperature [39]. This is also confirmed in Table 5 and Fig. 9. Additionally, the positive entropy (ΔS°) represents the increase of randomness at the solid/liquid interface during the adsorption of CFX on to the bio-char [38].

4. Conclusion

In the present study, pine cones is used as a natural raw material to prepare bio-char to remove CFX from aqueous solutions. Results showed that the appropriate yield = 35.5%; specific surface area = 789 m² g⁻¹; total pore volume = 0.373 cm³ g⁻¹; mean diameter = 1.89 nm, and pH_{pzc} = 6.5 in the prepared bio-char from dry raw pine cones. The bio-char successfully adsorbed CFX from aqueous solution at pH 6.3 with maximum monolayer adsorption capacities of 114.94 mg g⁻¹. In this study, with increasing adsorbent dose, the removal efficiency increased, and the adsorption capacity decreased significantly. The experimental data of CFX adsorption fitted very well to the Langmuir isotherm model.

The PSO kinetic model better described the adsorption kinetics. Recovery and reuse of the applied biosorbent in adsorption process are so important that should be considered in future research by other researchers. Overall, cefixime as a pollutant could be adsorbed from aqueous solutions by the activated carbons derived from pine cones through activation and can be used as an efficient adsorbent for the treatment of wastewater containing cephalosporin compounds such as CFX in hospitals and other health care centers.

Acknowledgments

This work was supported by Guilan and Babol University of Medical Sciences. The authors would like to thank all those who contributed to this work.

References

- [1] C.G. Daughton, T.A. Ternes, Pharmaceuticals and personal care products in the environment: agents of subtle change, *Environ. Health Perspect.*, 107 (1999) 907–938.
- [2] C. Pluss-Suard, A. Pannatier, A. Kronenberg, Hospital antibiotic consumption in Switzerland: comparison of a multicultural country with Europe, *J. Hosp. Infect.*, 79 (2011) 166–171.
- [3] M. Carballa, F. Omil, J.M. Lemma, M. Liompart, C. Garcia-Jares, I. Rodriguez, M. Gomez, T. Ternes, Behavior of pharmaceuticals, cosmetics and hormones in a sewage treatment plant, *Water Res.*, 38 (2004) 2918–2926.
- [4] F.I. Turkdogan, K. Yetilmezsoy, Appraisal of potential environmental risks associated with human antibiotic consumption in Turkey, *J. Hazard. Mater.*, 166 (2009) 297–308.
- [5] N. Alavi, A.A. Babaei, M. Shirmardi, A. Naimabadi, G. Goudarzi, Assessment of oxytetracycline and tetracycline antibiotics in manure samples in different cities of Khuzestan Province, Iran, *Environ. Sci. Pollut. Res.*, 22 (2015) 17948–17954.
- [6] M. Petrovic, S. Gonzalaez, D. Barcelo, Analysis and removal of emerging contaminants in wastewater and drinking water, *TrAC, Trends Anal. Chem.*, 22 (2003) 685–695.
- [7] M. Klavarioti, D. Mantzavinos, D. Kassinos, Removal of residual pharmaceuticals from aqueous systems by advanced oxidation processes, *Environ. Int.*, 35 (2009) 402–417.
- [8] T.A. Ternes, M. Bonerz, N. Herrmann, B. Teiser, H.R. Andersen, Irrigation of treated wastewater in Braunschweig, Germany: an option to remove pharmaceuticals and musk fragrances, *Chemosphere*, 66 (2007) 894–904.
- [9] Z. Fang, J. Chen, X. Qiu, W. Cheng, L. Zhu, Effective removal of antibiotic metronidazole from water by nanoscale zero-valent iron particles, *Desalination*, 268 (2011) 60–67.
- [10] S. Ata, A. Rasool, A. Islam, I. Bibi, M. Rizwan, M.K. Azim, A.R. Qureshi, M. Iqbal, Loading of cefixime to pH sensitive chitosan based hydrogel and investigation of controlled release kinetics, *Int. J. Biol. Macromol.*, 155 (2020) 1236–1244.
- [11] M. Abbas, M. Adil, S. Ehtisam-ul-Haque, B. Munir, M. Yameen, A. Ghaffar, *Vibrio fischeri* bioluminescence inhibition assay to toxicity assessment: a review, *Sci. Total Environ.*, 625 (2018) 1295–1309.

- [12] M. Iqbal, M. Abbas, J. Nisar, A. Nazir, A. Qamar, Bioassays based on higher plants as excellent dosimeters for ecotoxicity monitoring: a review, *Chem. Int.*, 5 (2019) 1–80.
- [13] A.Y.C. Lin, T.H. Yu, S.K. Lateef, Removal of pharmaceuticals in secondary wastewater treatment processes in Taiwan, *J. Hazard. Mater.*, 167 (2009) 1163–1169.
- [14] I. Belghadr, G. Shams Khorramabadi, H. Godini, M. Almasian, The removal of the CFX antibiotic from aqueous solution using an advanced oxidation process (UV/H₂O₂), *Desal. Water Treat.*, 58 (2014) 1–8.
- [15] M.H. Rasoulifard, S. Khanmohammadi, A. Heidari, Adsorption of cefexime from aqueous solutions using modified hardened paste of portland cement by perlite; optimization by Taguchi method, *Water Sci. Technol.*, 74 (2016) 1069–1078.
- [16] R. Khazaei, A. Rahmani, A. Seidmohammadi, J. Fardmal, M. Leili, Evaluation of the efficiency of photocatalytic UV/peroxy monosulfate process in the removal of cefexime antibiotic from aqueous solutions, *J. Kurdistan Univ. Med. Sci.*, 102 (2019) 22–40.
- [17] M.O. Uslu, I.A. Balcoglu, Comparison of the ozonation and fenton process performances for the treatment of antibiotic containing manure, *Sci. Total Environ.*, 407 (2009) 3450–3458.
- [18] F.J. Benitez, J.L. Acero, F.J. Real, G. Roldan, F. Casas, Comparison of different chemical oxidation treatments for the removal of selected pharmaceuticals in water matrices, *Chem. Eng. J.*, 168 (2008) 1149–1156.
- [19] A. Chatzitakis, C. Berberidou, I. Paspaltsis, G. Kyriakou, T. Sklaviadis, I. Poullos, Photocatalytic degradation and drug activity reduction of chloramphenicol, *Water Res.*, 42 (2008) 386–394.
- [20] M. Jafari, F. Aghamiri, G. Khaghanic, Batch adsorption of Cephalosporins antibiotics from aqueous solution by means of multi-walled carbon nanotubes, *World Appl. Sci. J.*, 14 (2011) 1642–1650.
- [21] Z. Aksu, O. Tunc, Application of biosorption for penicillin G removal: comparison with the activated carbon, *Process Biochem.*, 40 (2005) 831–847.
- [22] H. Liu, W. Liu, J. Zhang, C. Zhang, L. Ren, Y. Li, Removal of cephalaxin from aqueous solutions by original and Cu(II)/Fe(III) impregnated bio-chars developed from lotus stalks kinetics and equilibrium studies, *J. Hazard. Mater.*, 185 (2015) 1528–1535.
- [23] M.S. Legnoverde, S. Simonetti, E. Basaldella, Influence of pH on cephalaxin adsorption onto SBA-15 mesoporous silica: theoretical and experimental study, *Appl. Surf. Sci.*, 300 (2014) 37–42.
- [24] T.A. Cigu, S. Vasiliu, S. Racovita, C. Lionte, V. Sunel, M. Popa, C. Cheptea, Adsorption and release studies of new cephalosporin from chitosan-g-poly(glycidyl methacrylate) micro particles, *Eur. Polym. J.*, 82 (2016) 132–152.
- [25] H.R. Pouretdal, N. Sadegh, Effective removal of amoxicillin, cephalaxin, tetracycline and penicillin G from aqueous solutions using bio-char nanoparticles prepared from vine wood, *J. Water Process Eng.*, 1 (2014) 64–73.
- [26] M. Xia, A. Li, Z. Zhu, Q. Zhou, W. Yang, Factors influencing antibiotics adsorption onto engineered adsorbents, *J. Environ. Sci.*, 25 (2013) 1291–1299.
- [27] E.K. Putra, R. Pranowo, J. Sunarso, N. Indraswati, S. Ismadi, Performance of bio-char and bentonite for adsorption of amoxicillin from wastewater: mechanisms, isotherm and kinetics, *Water Res.*, 43 (2009) 2419–2430.
- [28] G. Nazari, H. Abolghasemi, M. Esmaili, Batch adsorption of cephalaxin antibiotic from aqueous solution by walnut shell-based bio-char, *J. Taiwan Inst. Chem. Eng.*, 58 (2016) 357–365.
- [29] D. Naghipour, A.I. Amouei, M. Estaji, K. Taghavi, Cephalaxin adsorption from aqueous solutions by bio-char prepared from plainain wood: equilibrium and kinetics studies, *Desal. Water Treat.*, 143 (2019) 374–381.
- [30] J. Rivera-Utrilla, G. Prados-Joya, M. Sanchez-Polo, M.A. Ferro-Garcia, I. Bautista-Toledo, Removal of nitroimidazole antibiotics from aqueous solution by adsorption/bioadsorption on bio-char, *J. Hazard. Mater.*, 170 (2009) 298–305.
- [31] A. Babarinde, K. Ogundipe, K. Tobi Sangosanya, B. Damilare Akintala, A.O.E. Hassan, Comparative study on the biosorption of Pb(II), Cd(II), Zn(II) using lemon grass (*Cymbopogon citratus*): kinetics, isotherms and thermodynamics, *Chem. Int.*, 6 (2016) 89–102.
- [32] S.N. Mohseni, A.A. Amooey, H. Tashakkorian, A.I. Amouei, Removal of dexamethasone from aqueous solutions using modified clinoptilolite zeolite (equilibrium and kinetic), *Int. J. Environ. Sci. Technol.*, 13 (2016) 2261–2268.
- [33] J. Torres-Perez, C. Gerente, Y. Andre, Sustainable bio-chars from agricultural residues dedicated to antibiotic removal by adsorption, *Chin. J. Chem. Eng.*, 20 (2012) 524–529.
- [34] N.E. Anderson Asoluka, Use of agro-waste (*Musa paradisiaca* peels) as a sustainable biosorbent for toxic metals ions removal from contaminated water, *Chem. Int.*, 4 (2018) 52–59.
- [35] M. Fazal-ur-Rehman, Methodological trends in preparation of activated carbon from local sources and their impacts on production: a review, *Chem. Int.*, 4 (2018) 109–119.
- [36] H. Wang, C. Fang, Q. Wang, Y. Chu, Y. Song, Y. Chenab, X. Xueab, Sorption of tetracycline on bio-char derived from rice straw and swine manure, *RSC Adv.*, 8 (2018) 16260–16268.
- [37] A.C. Martins, D. Pezoti, A.L.C. Cazetta, K.C. Bedlin, D.A.S. Yamazaki, Removal of tetracycline by NaOH-activated carbon produced from macadamia nut shells: kinetic and equilibrium studies, *Chem. Eng. J.*, 260 (2015) 291–299.
- [38] V. Hassanzadeh, O. Rahmadian, M. Heidari, Cefixime adsorption onto activated carbon prepared by dry thermochemical activation of date fruit residues, *Microchem. J.*, 152 (2020) 1–9.
- [39] A. Fakhri, S. Adami, Adsorption and thermodynamic study of Cephalosporins antibiotics from aqueous solution onto MgO nanoparticles, *J. Taiwan Inst. Chem. Eng.*, 45 (2014) 1001–1006.
- [40] R. Sudha, K. Srinivasan, P. Premkumar, Removal of nickel(II) from aqueous solution using *Citrus limettioides* peel and seed carbon, *Ecotoxicol. Environ. Saf.*, 117 (2015) 115–123.
- [41] H. Saygılı, F. Güzel, Effective removal of tetracycline from aqueous solution using activated carbon prepared from tomato (*Lycopersicon esculentum* Mill.) industrial processing waste, *Ecotoxicol. Environ. Saf.*, 131 (2016) 22–29.
- [42] M.S. Miao, Q. Liu, L. Shu, Z. Wang, Y.Z. Liu, Q. Kong, Removal of cephalaxin from effluent by activated carbon prepared from alligator weed: kinetics, isotherms, and thermodynamic analyses, *Process Saf. Environ. Prot.*, 104 (2016) 481–489.
- [43] M.E. Fernandez, B. Ledesma, S. Roman, P.R. Bonelli, A.L. Cukierman, Development and characterization of activated hydrochars from orange peels as potential adsorbents for emerging organic contaminants, *Bioresour. Technol.*, 183 (2015) 221–228.
- [44] E. Çalışkan, S. Göktürk, Adsorption characteristics of sulfamethoxazole and metronidazole on bio-char, *Sep. Sci. Technol.*, 45 (2010) 244–255.